HEAT TRANSFER INCREMENT STUDY TAKING INTO CONSIDERATION FIN LENGTHS FOR CuO-WATER NANOFLUID IN CROSS FLOW-IMPINGING JET FLOW CHANNELS

by

Koray KARABULUT*

Electric and Energy Department, Sivas Technical Science Vocational School,
Sivas Cumhuriyet University, Sivas, Turkey

Original scientific paper
https://doi.org/10.2298/TSCI221203035K

In this study, the heat transfer and flow characteristics for cube and circular hollow models in channels with the cross-flow-impinging jet-flow were numerically investigated by using water and 2% CuO-water nanofluid. The numerical work was carried out steady and 3-D using the ANSYS-FLUENT program with the k-ε turbulence model. A fin with 45° and 90° angles and D, 1.166 D, and 1.333 D (K) lengths was added to the upper channel surface from the impinging jet inlet at D (N) distance. A constant heat flux of 1000 W/m^2 was applied to the model surfaces. The channel height is fixed in 3D (H) and the Reynolds number range of the fluids is 5000-15000. The numerical results obtained from the study were compared with the results of the experimental study in the literature and it was seen that the results were compatible and acceptable. The results of the study were examined as the mean Nusselt number, surface temperature, and performance evaluation coefficient variations for each model in the channels. Also, velocity and temperature contour distributions of the combined jet CuO-water nanofluid flow were visualized. The average Nusselt number increases for CuO-water nanofluid at Re = 15000, K = D, and 90° fin angle are 32.55% and 26.11% compared to without fin and water fluid for cube and circular hollow models, respectively.

Key words: *cross-flow-impinging jet-flow, CuO-water nanofluid, fin length*

Introduction

The cross-flow cooling method, which is used to increase heat transfer from electronic elements, is one of the most widely used methods. This method is based on the principle of sending the cold fluid over all the components with a fan, thereby cooling the entire electronic components. Another method of heat transfer is impinging jet cooling where cold fluid is locally sprayed onto an element with a high temperature with a nozzle. For this reason, it is difficult to reach the conditions that can keep the whole circuit safely with a single type of cooling method. Implementing the impinging jet and cross-flow cooling method together can create a beneficial situation with high cooling capacity [1, 2].

In the literature, there are many studies evaluating only cross-flow or only jet-flow. Since the model examined for this study is more like jet-flow, the literature review focused more on jet-flow. However, there are many numerical and experimental studies on impinging jets in the literature. Karabulut and Alnak [3] numerically investigated the heat transfer from

* Author's e-mail: kkarabulut@cumhuriyet.edu.tr

the copper plate surfaces with different patterns as rampart and rectangular using a single air jet stream in rectangular cross-section channels, the distance between the jet and the plate (H/D_h) is between 4-10. As a result of their research, they found a 31.45% higher average Nusselt number value on rectangular patterned surfaces compared to rampart patterned surfaces for the value where the Reynolds number is 4000 and the distance between the jet and the plate is 4. Zou *et al.* [4] used high-speed compressed air impinging to research the interfacial heat transfer and gas-flow in the process of air-cooling in their experiment and numerical simulation. The effects of sample diameter and jet distance on the flow pattern and temperature field were studied. The results showed that the smaller the jet distance was the bigger the interfacial heat transfer coefficient. Demircan [5] numerically investigated the heat transfer from the electronic circuit element by cross-flow-impinging jet. It was concluded that the heat transfer increased significantly with the improvement of Reynolds number and velocity ratios. Heat transfer with impinging air jet-cross-flow coexistence on a constant heat flux element was investigated numerically by Ozturk and Demircan [6]. In their study, the researchers were investigated the heat transfer from a single element in the channel for different jet inlet velocity/channel inlet velocity ratios (0, 1, 2, and 3) and for different angles of the fins (0°, 22.5°, 45°, 67.5°, and 90°) placed in the duct, While the ratio of channel height to jet diameter was taken as constant and 3, the air was used as a fluid in the channel. It was determined that the highest heat transfer from the element was reached when the ratio of the inlet velocity to the channel inlet velocity was 3 and the fin angle was 90°.

When the jet impingement studies using nanofluids are examined, Kumar *et al.* [7] used a heat sink combined with airfoil columns in the jet impingement condition to increase the heat transfer rate. While doing this, they used water and CuO-water nanofluid with 1% concentration in their research. In their results, it was found a 10% reduction in heat sink temperature when they used water fluid as a jet fluid, while the temperature drop was 14% when they used nanofluid. Selimefendigil and Chamka [8] aimed to numerically analyze the convection heat transfer properties in cooling an isothermal surface with a cavity-like part using a CuO-water nanojet. They carried out their work by changing the volumetric concentration (0-4%) of the nanoparticle at different values of Reynolds number (100-400), different cavity lengths (5W-40W) and heights (W-5W). They found that the average heat transfer increases by 35-46% when nanofluid is used instead of water at the highest volumetric concentration. Abdullah *et al.* [9] experimentally investigated the effect of TiO_2 nanosolution concentration on the heat transfer of double jet impinging on an aluminium plate surface. Apart from this, the nozzle distance of the double jet and the nozzle-plate distance were considered variables. Based on these data, they found that the flow structure of the double jet is an important condition affecting the heat transfer increase. In addition, they determined that the distances and nanoparticle concentration, which affects the flow structure, also affect the Nusselt number together with the Reynolds number. Datta *et al.* [10] carried out a numerical simulation to investigate the heat transfer performance using Al_2O_3-water nanofluid (40 nm average particle size) in a confined slot jet impinging on a convex surface. In order to investigate the flow behavior and convective heat transfer performance of the system, different parameters such as various Reynolds numbers, and the distance between the jet and the plate were considered. They determined that the mean Nusselt number and heat transfer coefficient increased significantly with the increase in the jet inlet Reynolds number. They reached the highest increase of Nusselt number of 17% using nanofluid as compared to that of the base fluid.

As can be seen from the literature reviews, although there are many studies with impinging jets, the number of combined jet-flow studies in which the impinging jet and

cross-flow are applied together is quite low. However, the study used CuO-water nanofluid, which exhibits high heat transfer performance has not been found in the literature. In addition, when compared to the studies reached in the literature [7, 8, 11], for this study higher heat transfer rates against low-pressure drop have been achieved compared to the channels in which only the jet-flow CuO-water nanofluid is used. Besides, the main purpose of this study, the effect of the lengths of the different angled fins in the channel on the heat transfer from different shaped surfaces and the flow structure around the surfaces could not be found in the literature. In this study, flow characteristics and heat transfer from the cube and circular hollow model surfaces in combined jet-flow channels with $H = 3D$ height were analyzed numerically using water and 2% CuO-water nanofluid without fin and with a fin at 45° and 90° angles and fin lengths of $K = D$, $K = 1.166\ D$, and $K = 1.333\ D$, and $N = D$ fin distance from the impinging jet inlet. Numerical research was carried out by solving steady and 3-D energy and Navier-Stokes equations using the ANSYS-FLUENT program with the k-ε turbulence model. While the lower and upper surfaces of the fin and channel are adiabatic, the model surfaces have a constant heat flux of 1000 W/m^2, which is also applied in [12, 13]. The Reynolds number range studied for fluids is 5000-15000. These selected Reynolds number values have been chosen based on the studies in the literature and represent both the jet Reynolds number, $\mathrm{Re_j}$, and the channel Reynolds number, $\mathrm{Re_c}$. Fin lengths, angles and position of the fin have been chosen in dimensions that will not restrain the flow and heat transfer in the channel considering the studies in the literature. Thermophysical properties of CuO-water nanofluid with 2% volumetric concentration and 23.6 nm CuO particle size were found with the help of the equations found in the literature. The results of the study were compared with the experimental study in the literature and they were found to be compatible. The results were analyzed as the average Nusselt number variations for each cube and circular hollow model surface in the channels. However, velocity and temperature contour distributions of the CuO-water nanofluid in finless and with fin angles of 45° and 90° and fin length of 1.333 D for combined jet-flow channels were presented for Re = 13000. The mean Nusselt number, $\mathrm{Nu_m}$, and mean surface temperature, T_m, values were evaluated for all models found in the channels with Re = 5000 and Re = 15000 values in the finless and with different fin angles ($\theta = 45°$ and $\theta = 90°$) at $K = D$ fin length. In addition, the performance evaluation coefficient (PEC) was interpreted by considering the different fin angles and fin lengths for CuO-water nanofluid.

Thermophysical properties of CuO-water nanofluid

Thermophysical properties of solid CuO nanoparticle, CuO-water nanofluid with 2% volumetric concentration, and water were obtained with the help of equations found in [14] and widely used and shown in tab. 1. In addition, the thermophysical properties of the solid CuO nanoparticle and CuO-water nanofluid were also taken from the relevant study [15].

Specific heat of the CuO-water nanofluid:

$$c_{p,\mathrm{nf}} = (1-\varphi)c_{p,\mathrm{bf}} + \varphi c_{p,\mathrm{p}} \tag{1}$$

Density of CuO-water nanofluid:

$$\rho_{\mathrm{nf}} = (1-\varphi)\rho_{\mathrm{bf}} + \varphi\rho_p \tag{2}$$

Thermal conductivity of CuO-water nanofluid:

$$k_{\mathrm{nf}} = \frac{k_p + 2k_{\mathrm{bf}} + 2(k_p - k_{\mathrm{bf}})\varphi}{k_p + 2k_{\mathrm{bf}} - 2(k_p - k_{\mathrm{bf}})\varphi} k_{\mathrm{bf}} \tag{3}$$

Viscosity of CuO-water nanofluid:

$$\mu_{\mathrm{nf}} = \mu_{\mathrm{bf}}(1 + 2.5\varphi) \tag{4}$$

Table 1. Thermophysical properties of CuO nanoparticle, CuO-water, and water at 303 K [15]

Properties	Water	CuO-water nanofluid	CuO nanoparticle
Thermal conductivity, k [$\mathrm{Wm^{-1}K^{-1}}$]	0.6172	0.6639	20
Density, ρ [$\mathrm{kgm^{-3}}$]	995.8	1105.884	6500
Specific heat, c_p [$\mathrm{Jkg^{-1}K^{-1}}$]	4178.4	4105.54	535.6
Viscosity, μ [$\mathrm{Nsm^{-2}}$]	$803.4 \cdot 10^{-6}$	$843.57 \cdot 10^{-6}$	–

Numerical method

The ANSYS-FLUENT finite volume method program was used to solve the forced convection heat transfer of the combined jet-flow on the model surfaces. As a discretization method, the *Second order upwind* method for energy and momentum equations and the *First order upwind* method for turbulence equations were preferred. For the numerical solutions to converge, the convergence criterion was taken as 10^{-6} for the momentum, energy and turbulence equations. Flow and heat transfer were done by solutions of differential equations derived from the equations of conservation of mass, momentum and, energy for continuous, turbulent flow due to combined jet-flow in the channel, in which there is no body force, as follows [12, 13, 16].

Accurate modelling of turbulence is essential in heat transfer processes. However, direct numerical simulations of turbulent fluids are very difficult and also a time-consuming process. Although there are various turbulence models [17] used in numerical modelling among these models in terms of being economical and yielding results with acceptable accuracy in many flow events. The *k-ε* turbulence model, which is a semi-empirical model, is widely used [16]. Accordingly, considering the results obtained from the studies in the literature, the standard *k-ε* turbulence model was used for the channels in numerical calculations in this study.

Continuity equation:

$$\frac{\partial \overline{u}_i}{\partial x_j} = 0 \tag{5}$$

Momentum equation:

$$\rho \frac{\partial}{\partial x_j}(\overline{u}_i \overline{u}_j) = \frac{\partial \overline{p}}{\partial x_i} + \frac{\partial}{\partial x_j}\left[\mu\left(\frac{\partial \overline{u}_i}{\partial x_j} + \frac{\partial \overline{u}_i}{\partial x_j}\right) - \rho\overline{u_i' u_j'}\right] \tag{6}$$

Energy equation:

$$\rho c_p \frac{\partial}{\partial x_i}(\overline{u}_i \overline{T}) = \frac{\partial}{\partial x_i}\left[k\frac{\partial \overline{T}}{\partial x_i} - \rho c_p \overline{T' u_i'}\right] \tag{7}$$

Turbulence kinetic energy equation:

$$\frac{\partial}{\partial x_i}(\rho k u_i) + \frac{\partial}{\partial y}(\rho k) = \frac{\partial}{\partial x_j}\left[\mu + \frac{\mu_t}{\sigma_k}\frac{\partial k}{\partial x_j}\right] + G_k - \rho\varepsilon \tag{8}$$

Turbulence kinetic energy disappearance equation:

$$\frac{\partial}{\partial x_i}(\rho\varepsilon u_i) + \frac{\partial}{\partial y}(\rho\varepsilon) = \frac{\partial}{\partial x_j}\left[\left(\mu + \frac{\mu_t}{\sigma_\varepsilon}\right)\frac{\partial\varepsilon}{\partial x_j}\right] + C_{1\varepsilon}\frac{\varepsilon}{k}G_k - C_{2\varepsilon}\rho\frac{\varepsilon^2}{k} \tag{9}$$

where ρ is the density of the fluid, k – the kinetic energy of the turbulent flow, u_i – the velocity components in the x-, y-, and z-directions, μ – the viscosity of the fluid, and σ_k ($\sigma_k = 1$) – the turbulent kinetic energy Prandtl number. The equations showing turbulence kinetic energy production, G_k and turbulent viscosity, μ_t, are [12, 16]:

$$G_k = -\rho\overline{u_i' u_j'}\frac{\partial u_j}{\partial x_i} \tag{10}$$

$$\mu_t = C_\mu \rho\frac{k^2}{\varepsilon} \tag{11}$$

The turbulence disappearance Prandtl number is denoted by σ_ε, while $C_{1\varepsilon} = 1.44$, $C_{2\varepsilon} = 1.92$, $C_\mu = 0.09$, and $\sigma_\varepsilon = 1.3$ are coefficients in equations [18].

Heat transfer coefficient, h, and Nusselt number, are calculated with eqs. (12) and (13), respectively.

Heat transfer coefficient:

$$h = \frac{q''}{T_s - T_f} \tag{12}$$

Nusselt number:

$$-k_f\left(\frac{\partial T}{\partial n}\right)_s = h(T_f - T_s) \quad \text{and} \quad \mathrm{Nu} = \frac{h(3m)}{k_f} \tag{13}$$

where T_f and T_s are the average temperatures of the fluid and the model surface, respectively, k_f – the thermal conductivity of the fluid, $3m$ – the total surface length of the model with which the fluid is in contact, and h and h_m are the point and mean convective heat transfer coefficient along the model surface, respectively. However, n is the direction perpendicular to the surface and the model surface average Nusselt number, $\mathrm{Nu_m}$, is found from the equations given further in the text.

Model surface mean heat transfer coefficient:

$$h_m = \frac{1}{3m}\int_0^{3m} h\mathrm{d}x \tag{14}$$

Model surface mean Nusselt number:

$$\mathrm{Nu_m} = \frac{h_m(3m)}{k_f} \tag{15}$$

The hydraulic diameter of the channel:

$$D_{\mathrm{ch}} = \frac{4A_{\mathrm{c}}}{P_{\mathrm{c}}} = \frac{4HW}{2(H+W)} \tag{16}$$

where A_{c} and P_{c} are the cross-sectional area and perimeter of the channel, respectively, while the height and width of the channel are represented by H and W. Jet inlet diameter, D, is equal to circular inlet jet hydraulic diameter $D_{\mathrm{h,jet}}$.

The Reynolds numbers of the channel and the jet are determined using:

$$\mathrm{Re}_{\mathrm{c}} = \frac{\rho V_{\mathrm{c}} D_{\mathrm{ch}}}{\mu} \quad \text{and} \quad \mathrm{Re}_{\mathrm{j}} = \frac{\rho V_{\mathrm{j}} D_{\mathrm{j}}}{\mu} \tag{17}$$

where the channel and jet-flow velocities of the fluid are denoted by V_{c} and V_{j}, respectively.

The pressure drop, ΔP, is calculated by:

$$D_{\mathrm{ch}} = \frac{4A_{\mathrm{c}}}{P_{\mathrm{c}}} = \frac{4HW}{2(H+W)} \tag{18}$$

where ΔP is the pressure drop between the inlets and outlets of finless and finned ducts, f – the friction factor, and L – the length of the duct.

The *PEC*:

$$PEC = \frac{\dfrac{\mathrm{Nu}_{\text{m-finned}}}{\mathrm{Nu}_{\text{m-finless}}}}{\dfrac{\Delta P_{\text{finned}}}{\Delta P_{\text{finless}}}} \tag{19}$$

Model geometries

While the dimensions of the impinging jet-cross-flow combined jet-flow finned channels and the models with cube and circular hollow model surfaces and fin geometry in the channels are given in fig. 1, dimensions of the channels are given in tab. 2 [6]. In addition, the assumptions and boundary conditions made in this study are presented in tab. 3. In addition, the regular tetrahedral mesh structure was used in the numerical calculations of the combined jet-flow channels.

Table 2. Dimensions of the channel and fin placement [6]

Parameter	Size	Parameter	Size
D	15 mm	m	20 mm
L	66 D	θ	45° and 90°
W	4 D	N	D
H	3 D	K	D, 1.166 D and 1.333 D

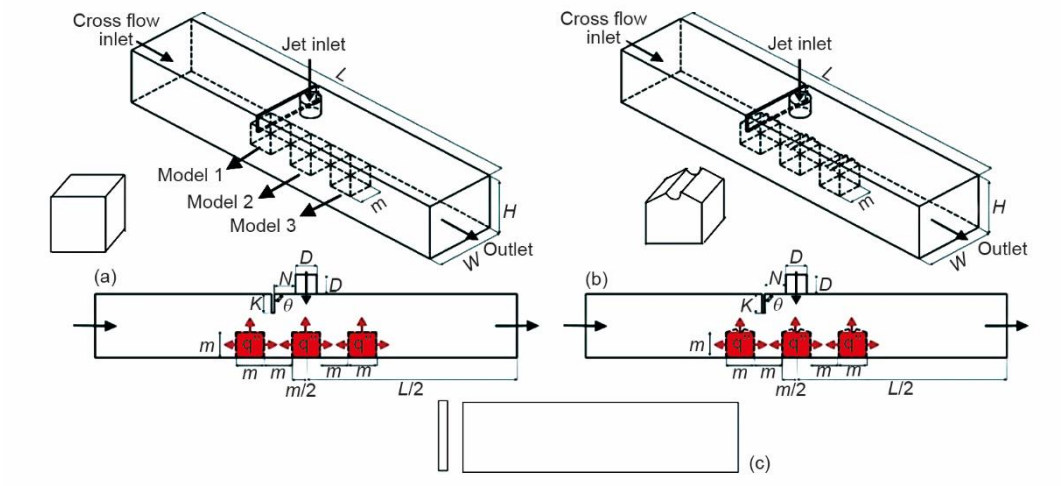

Figure 1. Views of channels with; (a) cube, (b) circular hollow model surfaces, and (c) fin geometry

Table 3. Assumptions and boundary conditions

a)	Steady, 3-D and turbulent flow volumes were used.
b)	Water and 2% CuO-water nanofluid used as incompressible fluids were both jet and cross-flow fluids.
c)	The thermal properties of the fluids are constant and independent of temperature.
d)	The surfaces of the channel and the fin are adiabatic.
e)	No heat source on water, nanofluid and model surfaces.
f)	The outlet pressure of the duct was taken as equal to the atmospheric pressure ($p_o = p_{atm}$).
g)	It was determined as $\partial T/\partial x = 0$ assuming that the temperature difference at the exit of the channel was negligible.
h)	It was assumed that there is a non-slip boundary condition on the channel, fin and model surfaces, and therefore, all velocity component values on the mentioned surfaces are zero.

Findings and discussions

In the study, as shown in fig. 2, the results obtained by examining different Reynolds numbers in the case of only jet-flow and by using the eq. (20) as a result of the experimental investigations of Ma and Bergles [19] were compared among themselves, and it was determined that the experimental results of Ma and Bergles [19] and the numerical results of the presented study were compatible and consistent.

$$\overline{\mathrm{Nu}} = 1.29\,\mathrm{Re}^{0.5}\,\mathrm{Pr}^{0.4} \tag{20}$$

In the study, the numerical results of this study were compared with the experimental study of the turbulent flow around a cube exposed to cross-flow and impinging jet combined flow by Masip *et al.* [20] and it was pointed out in fig. 3. Masip *et al.* [20] placed a cube-shaped model in a 2000 × 300 × 30 mm channel in their study. Assuming that all surfaces of the channel were taken adiabatically, by taking the ratio of the jet Reynolds number, $\mathrm{Re_j}$, to the channel Reynolds number, $\mathrm{Re_c}$, equal ($\mathrm{Re_j}/\mathrm{Re_c} = 1$), the flow structures around the elec-

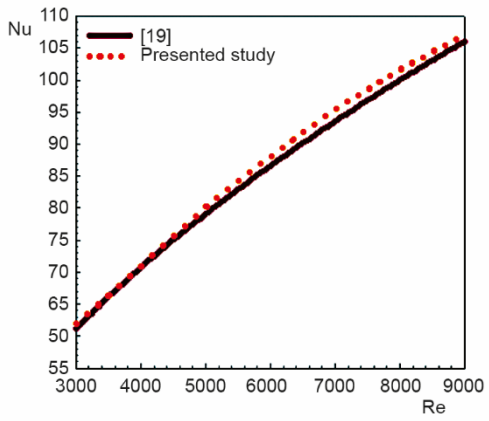

Figure 2. Comparison of the presented study and the results of [19]

tronic model were investigated at various positions (x/h). As can be seen in fig. 3, it was determined that the velocity profiles obtained as a result of the experimental study conducted by Masip *et al.* [20] were quite compatible with the presented study velocity profiles.

Provided that the variation of Nusselt number depending on the mesh number was determined. By specifying the most suitable number of mesh elements in the channel, the effect of mesh number on the average Nusselt number, Nu_m, in the finless combined jet-flow channel was presented in tab. 4 at different Reynolds numbers. Accordingly, it was found that 2022840 mesh elements will give reliable and accurate results for the finless channel.

Table 4. Variation of Nu_m with Reynolds number depending on the number of mesh elements

Mesh number	Re = 5000 Nu_m	Re = 7000 Nu_m	Re = 9000 Nu_m
1758412	86.48	108.84	127.40
2022840	86.52	108.88	127.43
2245786	86.52	108.87	127.42

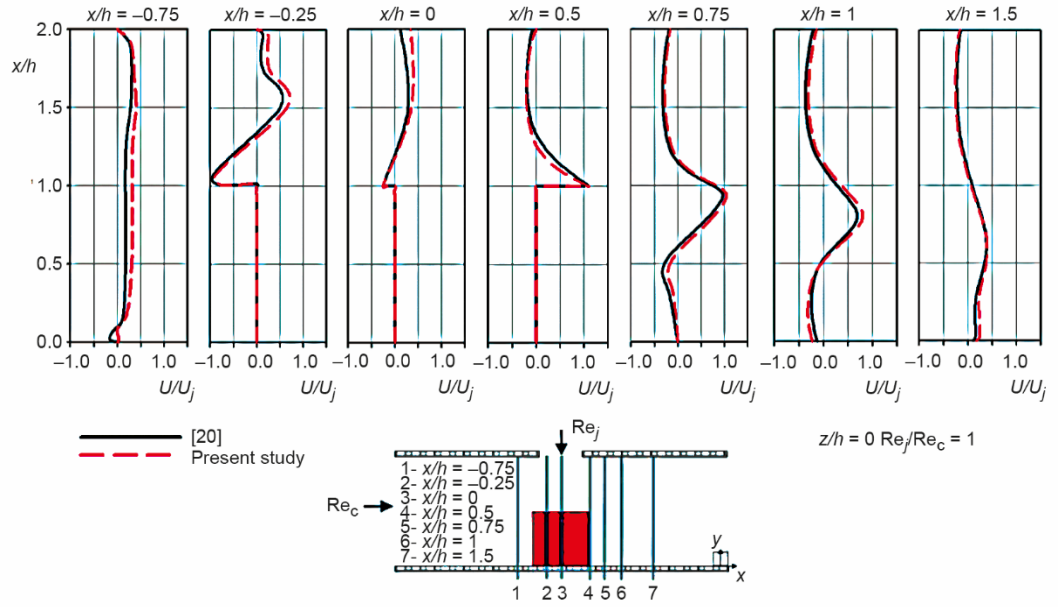

Figure 3. Comparison of the presented study and the experimental results of [20]

The mean Nusselt number variations of the cube and circular hollow model surfaces according to model rows in channels having cross-flow-impinging jet-flow without fin and

with fin angles of 45° and 90° at a D distance (N) from the impinging jet inlet and fin lengths of D, 1.166 D, and 1.333 D (K) by using water and 2% CuO-water nanofluids are shown in figs. 4(a) and 4(b), respectively. For the Model 1 surfaces, it is seen that adding fins to the channels according to the finless situation leads to an increase in the Nusselt number since it directs the cross-flow to the model surfaces. However, since the fin angle is 90°, it increases the fluid velocity on the surfaces by narrowing the cross-flow passage, thus increasing the Nusselt number by more than 45°. In addition, as a prominent issue, the increase in the fin length not only provides better orientation of the fluid on the surfaces but also increases heat transfer by activating the fluid between the models. Therefore, for Re = 11000, increasing the fin length from D to 1.333 D (K) at a 90° fin angle for cube Model 1 provides an 8.77% increase in Nusselt number. This increased value is 11.26% for the circular hollow Model 1. When the Model 2 surfaces are examined, it can be seen from figs. 4(a) and 4(b) that the average Nusselt number values reached are higher than that of Model 1, since they are also under the influence of the impinging jet-flow in addition to the cross-flow. However, the fact that CuO nanoparticles added to the fluid increase the heat transfer surface area and that the velocity boundary layer is flatter on the model surfaces and flatter in the channel center with its turbulent effect in the fluid, thinning the thermal boundary layer on the model surfaces, providing an effect of increasing heat transfer and improving the cooling performance of the surfaces [21-24]. This situation can be understood from the velocity increases and temperature variations of the fluid on the model surfaces in the velocity contour distributions in fig. 6. For Re = 15000, at K = 1.166 and 45° fin angle, the Nusselt number increase is 23.95% for cube Model 2 compared to Model 1. This value is 19.32% for the circular hollow model. Since the Model 3 surfaces are the surfaces where the effect of the combined jet-flow decreases, the Nusselt number values are lower compared to Model 2, but the Nusselt number values are higher compared to Model 1. While there is an 8% decrease in Nusselt number from Model 2 to Model 3 for $K = D$ in Re = 9000 and circular hollow model in 90°, this value is 15.15% higher for Model 3 than Model 1. Although equivalent results are obtained for the cube model, the decrease and increase values of the Nusselt number, respectively, are higher for Model 3 than for the circular hollow model, according to Model 2 and Model 1. It is seen that the Nusselt number increases achieved in this study are higher when compared to TiO_2-Su [9], CuO-Su [7, 8, 11], and Al_2O_3-Su [10] nanofluids reached in the literature. In general, different nanofluids with only jet fluid have been used in the studies, and the Nusselt number is around 14% to 17%. Although a higher Nusselt number value can be obtained depending on the nanoparticle concentration and Reynolds number, it can be said that the cross-flow-impinging jet-flow heat transfer method is more effective when the concentration used in this study is considered.

Mean Nusselt number, Nu_m, and mean surface temperature, T_m, values for all three cube and circular hollow model surfaces in the combined jet-flow channels at $H = 3D$ channel height and the Reynolds number values of 5000 and 15000 are given in tab. 5 without fin and with fin angles of 45° and 90° and, $K = D$ fin length, respectively. Since CuO-water nanofluid has higher thermal conductivity than water fluid, it has a higher heat transfer coefficient in forced convection jet-flows than water. Therefore, Nu_m number values are higher in cross-flow-impinging jet-flow channels using nanofluids. Besides, as the nanoparticles in the fluid increase the interaction between the model surface and the water, which is the base fluid, it causes an improving effect on the heat transfer performance. The Nu_m increases for

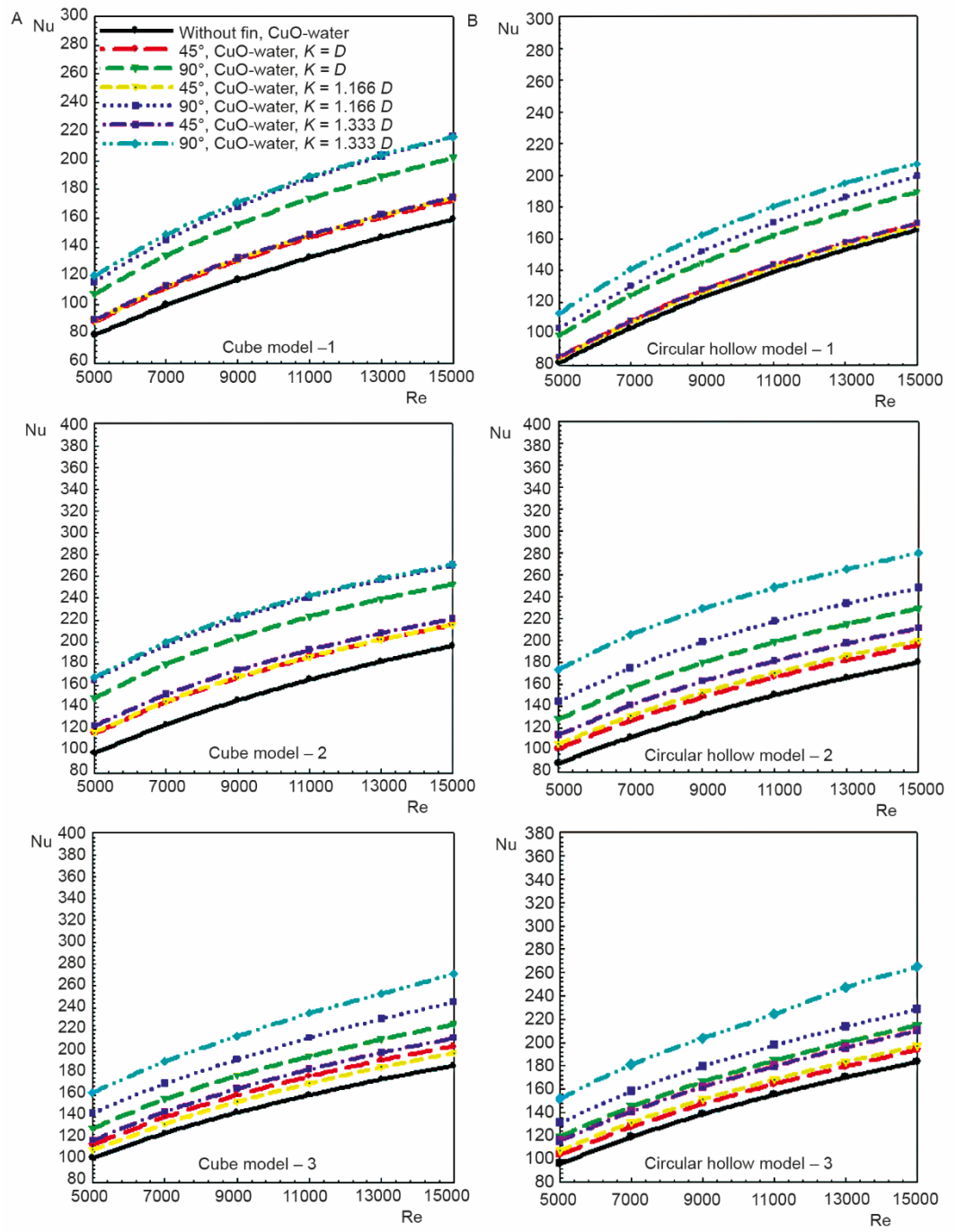

Figure 4. Variation of mean Nusselt number with Reynolds number according to model rows in cross-flow-impinging jet-flow channels with A-cube model and B-circular hollow model

Table 5. Results of Nu_m and T_m values by using water and CuO-water nanofluid at $K = D$

			Re = 5000		Re = 15000	
			Cube model	Circular hollow model	Cube model	Circular hollow model
Without fin	Water	Nu_m	86.523	82.872	170.964	167.493
Without fin	CuO-water	Nu_m	93.184	88.789	180.796	176.311
45° fin	Water	Nu_m	99.313	91.580	187.971	177.801
90° fin	Water	Nu_m	120.324	108.303	216.526	200.829
45° fin	CuO-water	Nu_m	106.574	96.955	197.665	186.239
90° fin	CuO-water	Nu_m	128.633	115.829	226.627	211.231
Without fin	Water	T_m [K]	306.634	306.768	304.130	304.223
Without fin	CuO-water	T_m [K]	306.180	306.393	303.978	304.086
45° fin	Water	T_m [K]	306.272	306.494	304.040	304.138
90° fin	Water	T_m [K]	305.344	305.613	303.748	303.85
45° fin	CuO-water	T_m [K]	305.869	306.045	303.903	303.973
90° fin	CuO-water	T_m [K]	305.043	305.265	303.647	303.716

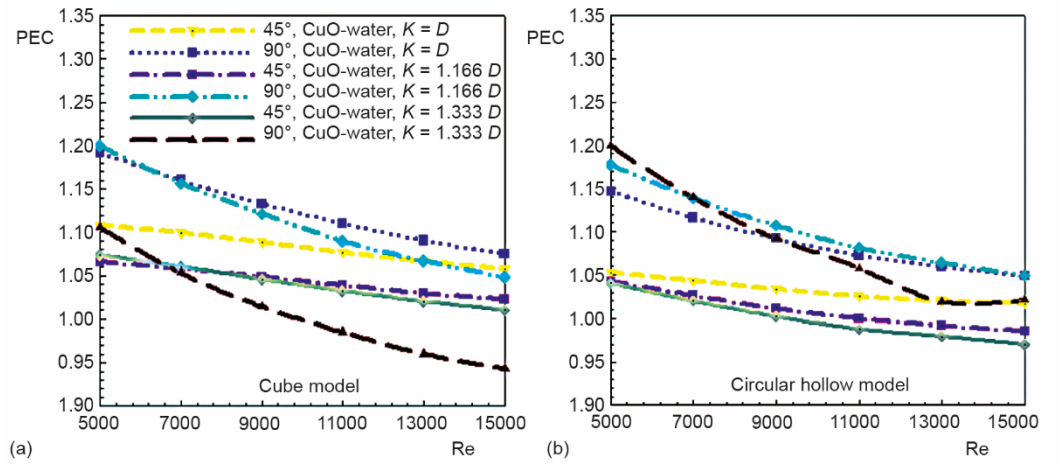

Figure 5. Variations of PEC with Reynolds number for fin lengths of $K = D$, $K = 1.166\ D$ and, $K = 1.333\ D$ in cross-flow-impinging jet-flow channels with (a) cube model and (b) circular hollow model

CuO-water nanofluid at Re = 15000, $K = D$ and, 90° fin angle are 32.55% and 26.11% compared to without fin and water fluid for cube and circular hollow models, respectively. In addition, for Re = 5000, the Nu_m is 20.7% and 19.47% higher, respectively, in the channels in which 90° fin angle and nanofluid are used, compared to 45° fin angle in the channels in which cube and circular hollow models are used. In the case of using fins in both model surface channels. The Nu_m numbers increase while T_m values decrease. While the highest temperature values are obtained for using water fluid and without fin, the lowest temperature values are observed for a fin angle of 90° and using CuO-water nanofluid.

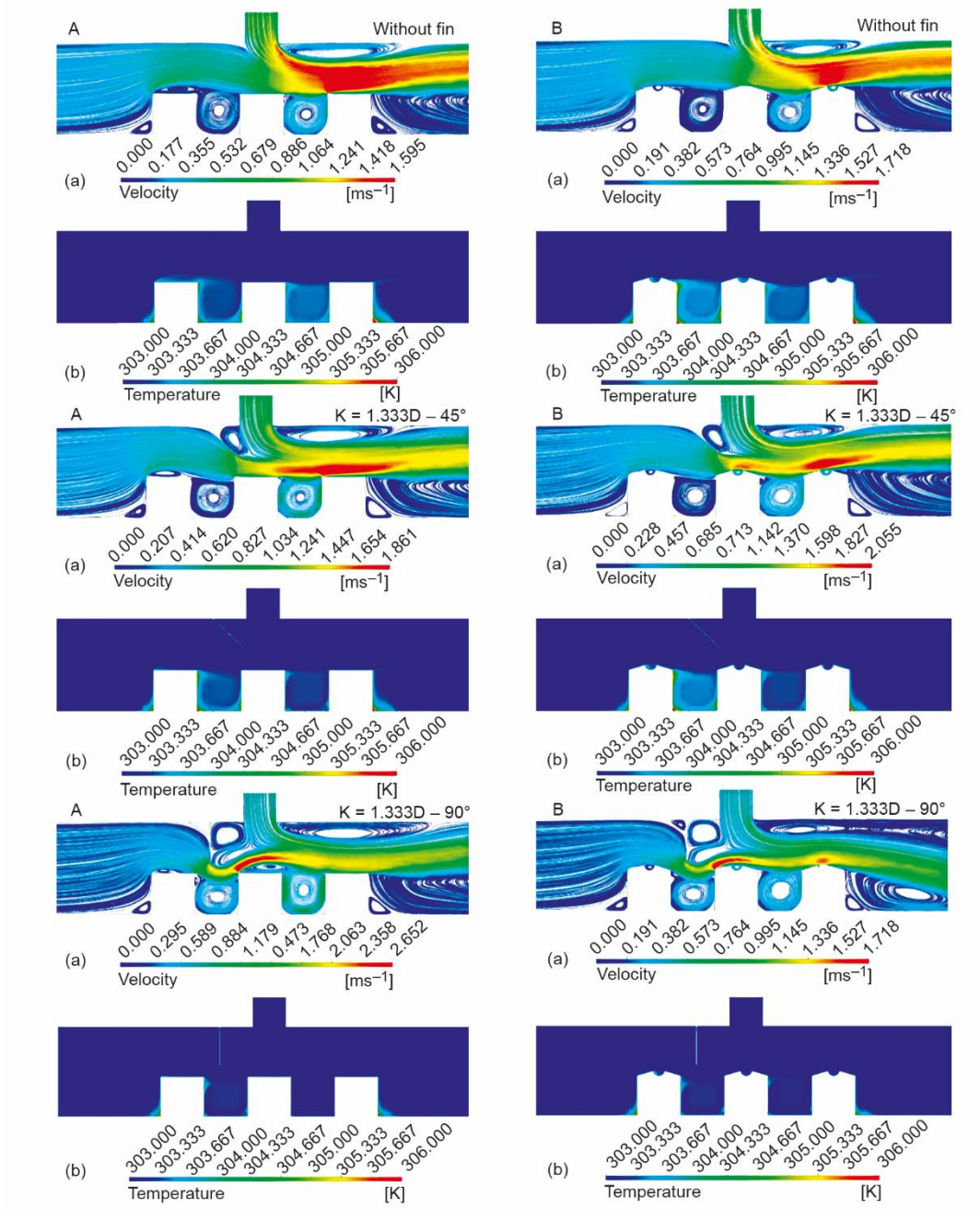

Figure 6. (a) Velocity and (b) temperature contour distributions in cross-flow-impinging jet-flow channels with A-Cube and B-Circular hollow model for CuO-water nanofluid

The PEC in the combined jet-flow channels using water and 2% CuO-water nanofluids belonging to the cube and circular hollow model surfaces are given according to different

fin lengths in figs. 5(a) and 5(b), respectively. The PEC shows the average Nusselt number increase performance *vs.* the pressure drop increase compared to the finless condition when using fins in combined jet-flow channels. For the cube model, the highest PEC is obtained for the 90° and $K = D$ fin length, while for the circular hollow model it is 90° and $K = 1.166\,D$. This difference in cross-flow-impinging jet-flow channels is due to the movement of the fluid in the channel, depending on the fin length and the pattern surface shape. For $K = D$ at Re = 15000, the PEC obtained for the cube model surface is 2.47% higher than the circular hollow model surface.

On fig. 6, are presented contour distributions of velocity (a) and temperature (b) of A-cube and B-circular hollow model surfaces in channels using CuO-water nanofluid, for the cases of using without a fin, 45° and 90° angled fins at fin length of $K = 1.333\,D$ and Re = 13000, respectively. As can be seen from the velocity contour distributions on Model 1, the fluid velocity is lower than in the circular hollow model due to the recirculation zones in the cube model. In addition to the cross-flow on Model 2, there is also the impinging jet-flow, which increases the nanofluid velocity in this model. On Model 3, the cross-flow-impinging jet-flow effect is seen better, and the flow acceleration on the model increases. When the temperature contour distributions are examined, the cooling increases in the regions where the nanofluid velocity increases. The addition of fins (with fin angles of 45° and 90°) to the channels, in particular, directs the cross-flow from the channel entrance to the model surfaces, increasing the heat transfer. The effect of both the fin angle and the length provides a better influence on the cube model than on the circular hollow model in terms of better contact of the fluid on the cube model surfaces.

Conclusions

In this study, the heat transfer and flow structures for the cube and circular hollow model copper surfaces in the cross-flow-impinging jet-flow channels with $H = 3D$ height were numerically analyzed taking into consideration without fin and with fin angles of 45° and 90° and, fin distances of $K = D$, $1.166\,D$ and $1.333\,D$ and also, fin arranged from the impinging jet inlet as $N = D$. While a constant heat flux of 1000 W/m^2 was applied to the model surfaces, water and CuO-water nanofluid with a volumetric concentration of 2%, respectively, were used as fluids in the channels. As a result of this study, while a detailed examination of the cross-flow-impinging jet-flow using different fin angles, fin lengths, and CuO-water nanofluid was made, the obtained results can be summarized as follows.

- For Re = 11000, increasing the fin length from D to $1.333\,D$ at a 90° fin angle for cube Model 1 provides an 8.77% increase in Nusselt number. This increase value is 11.26% for the circular hollow Model 1.
- For Re = 15000, at $K = 1.166$ and 45° fin angle, the Nusselt number increase is 23.95% for cube Model 2 compared to Model 1. This value is 19.32% for the circular hollow model. In Model 2, with the application of impinging jet-flow in addition to the cross-flow, the thermal boundary-layer thickness, where heat transfer takes place, is reduced and the heat transfer is increased.
- Since the Model 3 surfaces in the last row of the channel are the surfaces where the effect of the combined jet-flow decreases, the Nusselt number values are lower compared to Model 2, but the Nusselt number values are higher compared to Model 1. While there is an 8% decrease in Nusselt number from Model 2 to Model 3 for $K = D$ in Re = 9000 and circular hollow model in 90°, this value is 15.15% higher for Model 3 than Model 1.

- The CuO-water nanofluid has higher thermal conductivity than water fluid, which provides to have higher heat transfer coefficient in forced convection jet-flows than water. Therefore, Nu_m values are higher for nanofluid. In addition, as the nanoparticles in the fluid increase the interaction between the model surface and the water, which is the base fluid, it causes an improving effect on the heat transfer performance.
- The Nu_m increases for CuO-water nanofluid at Re = 15000, $K = D$ and, 90° fin angle are 32.55% and 26.11% compared to without fin and water fluid for cube and circular hollow models, respectively.
- In addition, for Re = 5000, the Nu_m is 20.7% and 19.47% higher, respectively, in the channels in which 90° fin angle and nanofluid are used, compared to the channels with an angle of 45°, in the channels in which cube and circular hollow models are used.
- While the highest temperature values are obtained for using water fluid and without a fin, the lowest temperature values are observed in the combined jet-flow channel with a fin angle of 90° and using CuO-water nanofluid.
- For the cube model, the highest PEC is obtained for the 90° and $K = D$ fin length, while for the circular hollow model it is 90° and $K = 1.166\,D$. Generally, lower PEC are observed for the channels with 45° angles for both model surfaces, while PEC decrease depending on the increase in pressure drop with increasing Reynolds number. For $K = D$ at Re = 15000, the PEC obtained for the cube model surface is 2.47% higher than the circular hollow model surface.
- Increasing the fin angle from 45° to 90° narrows the cross-sectional area of the fluid on the model surfaces, increasing the jet effect, while at the same time, it increases the cooling capacity of the surfaces by activating the fluid between the models.
- In addition to this, increasing the fin length from D to $1.333\,D$ provides a positive effect in terms of both enabling the fluid to move on the model surfaces and activating the recirculation zones, in addition to improving the flow mixing in the channel.
- The effect of both the fin angle and the length provides a better influence on the cube model than on the circular hollow model in terms of better contact of the fluid on the cube model surfaces.
- As a result, increasing the heat transfer from the patterned surfaces in the combined jet-flow channels is of great importance in terms of the operation of the circuit within safe temperature limits. In this case, apart from the pattern shape of the surfaces, the fin setup and placement used to direct the fluid in the channel to the model surfaces, the channel and jet Reynolds numbers and the thermophysical properties of the fluid are the main factors.

Acknowledgment

This study was supported by Sivas Cumhuriyet University Scientific Research Projects (CUBAP) unit with project number TEKNO-2021-031.

Nomenclature

A_c – cross-sectional area of the channel, [m^2]
c_p – specific heat of the fluid [$Jkg^{-1}K^{-1}$]
D – jet inlet diameter, [mm] [ms^{-1}]
f – friction factor, [–]
h – heat convection coefficient, [$Wm^{-2}K^{-1}$]
H – height of the channel, [mm]
K – fin length, [mm]
k – kinetic energy of turbulent flow, [m^2s^{-2}]
k_f – thermal conductivity of the fluid, [$Wm^{-1}K^{-1}$]
L – length of the channel, [mm]
m – one side length of the model, [mm]
N – distance of fin from jet inlet, [mm]
Nu – Nusselt number, (= hm/k_f), [–]
$\bar{p}$ – pressure, [Pa]

P_c – wet area of the channel, [m^2]
q'' – heat flux on model surfaces, [Wm^{-2}]
Re – Reynolds number, (= $\rho VD/\mu$), [–]
T – temperature, [K]
U – local velocity component at different x/h positions, [ms^{-1}]
U_j – local jet component at different x/h positions, [ms^{-1}]
u_i – velocity components in x-, y- and z-co-ordinates
V – velocity of the fluid at the inlet of the channel, [ms^{-1}]
W – width of the channel, [mm]

Greek symbols

μ – dynamic viscosity, [kgs^{-1}m^{-1}]
μ_t – turbulent viscosity, [kgs^{-1}m^{-1}]
θ – fin angle, [°]
ν – kinematic viscosity, [m^{2}s^{-1}]
ρ – density of the fluid, [kgm^{-3}]
ε – turbulent dissipation rate, [m^{2}s^{-3}]
φ – nanoparticle, volumetric concentration

Subscripts

bf – base fluid (water)
c – channel
f – fluid
h – hydraulic
j – jet
m – mean
nf – nanofluid
p – nanoparticle
s – surface

References

[1] Kilic, M., Investigation of Combined Effect of Nanofluids and Impinging Jets on Cooling of Electronic Systems, *Cukurova University Journal of the Faculty of Engineering Architecture, 18* (2018), Sept., pp. 121-132
[2] Teamah, M. A., *et al*., Numerical and Experimental Investigation of Flow Structure and Behavior of Nanofluids Flow Impingement on Horizontal Flat Plate, *Experimental Thermal Fluid Science*, *74* (2015), June, pp. 235-246
[3] Karabulut, K., Alnak, D. E., Study of Cooling of the Varied Designed Warmed Surfaces with an Air Jet Impingement, *Pamukkale University Journal of Engineering Science*, *26* (2020), 1, pp. 88-98
[4] Zou, L., *et al*., Evaluation of Interfacial Heat Transfer Coefficient Based on the Experiment and Numerical Simulation in the Air-Cooling Process, *Heat and Mass Transfer*, *58* (2022), 2, pp. 337-354
[5] Demircan, T., Numerical Analysis of Cooling An Electronic Circuit Component with Cross-flow and Jet Combination, *Journal of Mechanics*, *35* (2019), 3, pp. 395-404
[6] Ozturk, S. M., Demircan, T., Numerical Analysis of the Effects of Fin Angle on Flow and Heat Transfer Characteristics for Cooling an Electronic Component with Impinging Jet and Cross-Flow Combination, *Journal of the Faculty of Engineering and Architecture of Gazi University*, *37* (2022), 1, pp. 57-74
[7] Kumar, D., *et al*., Heat Sink Analysis in Jet Impingement with Air Foil Pillars and Nanoparticles, *Materials Today: Proceedings*, *46* (2021), 20, pp. 10752-10756
[8] Selimefendigil, F., Chamkha, A. J., Cooling of an Isothermal Surface Having a Cavity Component by Using Cuo-Water Nano-Jet, *International Journal of Numerical Methods Heat & Fluid Flow*, *30* (2020), 4, pp. 2169-2191
[9] Abdullah, M. F., *et al.*, Impact of the TiO_2 Nano Solution Concentration on Heat Transfer Enhancement of the Twin Impingement Jet of a Heated Aluminum Plate, *Micromachines*, *10* (2019), 3, 176
[10] Datta, A., *et al*., Heat Transfer Analysis of Slot Jet Impingement using Nano-Fluid on Convex Surface, *Proceedings*, *2nd* International Conference on Advances in Mechanical Engineering (ICAME 2018) Kattankulathur, India, 2018, Vol. 402, pp. 1-6
[11] Kareem, Z. S., *et al.*, Heat Transfer Enhancement in Single Circular Impingement Jet by CuO-water Nanofluid, Case Studies in Thermal Engineering, *15* (2019), Nov., 100508
[12] Kilic, M., *et al*., Experimental and Numerical Study of Heat Transfer from a Heated Fat Plate in a Rectangular Channel with an Impinging Air Jet, *Journal of the Brazilian Society of Mechanical Sciences and Engineering*, *39* (2016), Mar., pp. 329-344
[13] Karabulut, K., Heat Transfer Improvement Study of Electronic Component Surfaces using Air Jet Impingement, *Journal of Computational Electronics*, *18* (2019), 4, pp. 1259-1271
[14] Maxwell, J. C., *A Treatise on Electricity and Magnetism*, Clarendon Press, Oxford, UK, 1873
[15] Mohammed, H. A., *et al*., The Impact of Various Nanofluid Types on Triangular Microchannels Heat Sink Cooling Performance, *International Communications in Heat and Mass Transfer*, *38* (2011), 6, pp. 767-773

[16] Wang, S. J., Mujumdar, A. S., A Comparative Study of Five Low Reynolds Number *k-ε* Models for Impingement Heat Transfer, *Appield Thermal Engineering*, *25* (2005), 1, pp. 31-44
[17] Genc, M. S., *et al*., Flow over an Aerofoil without and with a Leading-Edge Slat at a Transitional Reynolds Number, *Proceedings of the Institution of Mechanical Engineers, Part G: Journal of Aerospace Engineering*, *223* (2009), 3, pp. 217-231
[18] Saleha, N., *et al*., Improving Cooling Effectiveness by use Chamfers on the Top of Electronic Components, *Microelectronic Reliability*, *55* (2015), 7, pp. 1067-1076
[19] Ma, C. F., Bergles, A. E. Boiling Jet Impingement Cooling of Simulated Microelectronic Chips, *Heat Transfer Electronic Equipment HTD*, *28* (1983), 1983, pp. 5-12
[20] Masip, Y., *et al*., Experimental Study of the Turbulent Flow Around a Single Wall-Mounted Cube Exposed to a Cross-Flow and an Impinging Jet, *International Journal of Heat and Fluid Flow*, *38* (2012), Dec., pp. 50-71
[21] Bhatti, M. M., *et al.,* Magnetic Nanoparticles for Drug Delivery through Tapered Stenosed Artery with Blood Based Non-Newtonian Fluid, *Pharmaceuticals*, *15* (2022), 11, 1352
[22] Ellahi, R., *et al.,* Numerical Simulation and Mathematical Modeling of Electro-Osmotic Couette–Poiseuille Flow of MHD Power-Law Nanofluid with Entropy Generation, *Symmetry*, *11* (2019), 8, 1038
[23] Ali Abro, K., *et al.,* Effects of Carbon Nanotubes on Magnetohydrodynamic Flow of Methanol Based Nanofluids *via* Atanganabaleanu and Caputo-Fabrizio Fractional Derivatives, *Thermal Science*, *23* (2019), 2B, pp. 883-898
[24] Ellahi, R. The Effects of MHD and Temperature Dependent Viscosity on the Flow of Non-Newtonian Nanofluid in A Pipe: Analytical Solutions, *Applied Mathematical Modelling*, *37* (2013), 3, pp. 1451-1467

Paper submitted: December 3, 2022
Paper revised: January 11, 2023
Paper accepted: January 19, 2023